

Immunocytochemistry and Distribution of Parabrachial Terminals in the Lateral Geniculate Nucleus of the Cat: A Comparison With Corticogeniculate Terminals

ALEV ERIŞİR, SUSAN C. VAN HORN, MARTHA E. BICKFORD,
AND S. MURRAY SHERMAN*

Department of Neurobiology, State University of New York,
Stony Brook, New York 11794-5230

ABSTRACT

We used immunohistochemistry in cats to demonstrate the presence of brain nitric oxide synthase (BNOS) in cholinergic fibers within the A-laminae of the lateral geniculate nucleus. We used a double labeling procedure with electron microscopy and found that all terminals labeled for choline acetyltransferase (ChAT) in the geniculate A-laminae were double labeled for BNOS. Also, some interneuron dendrites, identified by labeling for γ -aminobutyric acid (GABA), contained BNOS, but relay cell dendrites did not. We then compared parabrachial and corticogeniculate terminals, identifying the former by BNOS/ChAT labeling and the latter by orthograde transport of biocytin injected into cortical area 17, 18, or 19. All corticogeniculate terminals and most BNOS- or ChAT-positive brainstem terminals displayed RSD morphology, whereas some brainstem terminals exhibited RLD morphology. However, parabrachial terminals were larger, on average, than corticogeniculate terminals. We also found that parabrachial terminals were located both inside and outside of glomeruli, and they always contacted relay cell dendrites proximally among retinal terminals (the retinal recipient zone). In contrast, the cortical terminals were limited to peripheral dendrites (the cortical recipient zone). Thus, little if any overlap exists in the distribution of parabrachial and corticogeniculate terminals on the dendrites of relay cells. *J. Comp. Neurol.* 377:535-549, 1997. © 1997 Wiley-Liss, Inc.

Indexing terms: nitric oxide; acetylcholine; thalamus; BNOS; ChAT

The lateral geniculate nucleus provides the main transfer of retinal information to the cortex, but it is not a simple transfer (for reviews, see Singer, 1977; Burke and Cole, 1978; Sherman and Koch, 1986, 1990; Sherman, 1993). Relay cells themselves display a number of voltage-dependent membrane conductances, and the combination activated at any time plays a major role in how these cells respond to, and thus transmit, their retinal inputs to the cortex. Furthermore, these relay cells are embedded in very complex circuitry and receive only a minority of their inputs from the retina. Nonretinal inputs include local inhibitory inputs and a variety of inputs from extrathalamic sources, such as the cortex and brainstem. These nonretinal inputs play a major role in controlling the nature of the relay through the lateral geniculate nucleus, and understanding their functional organization is a key to understanding the function of this thalamic relay.

The largest of the extrathalamic, nonretinal inputs is the corticogeniculate pathway that emanates from glutamatergic cells in layer 6 of the visual cortex (Jones and Powell, 1969b; Guillery, 1969a; Gilbert and Kelly, 1975; Wilson et al., 1984; Montero, 1994). The other major such input is the cholinergic input that derives from cells in the midbrain parabrachial region, which lies in the vicinity of the brachium conjunctivum (de Lima and Singer, 1987b; Steriade et al., 1988; Fitzpatrick et al., 1989). The purpose of this study was to address two outstanding issues regarding these inputs.

Contract grant sponsor: USPHS; Contract grant numbers: EY03038, EY06473.

*Correspondence to: S. Murray Sherman, Department of Neurobiology, State University of New York, Stony Brook, NY 11794-5230. E-mail: ssherman@brain.bio.sunysb.edu

Received 11 June; Revised 27 September 1996; Accepted 21 October 1996

First, a recent report demonstrated that NADPH-diaphorase is colocalized among the cholinergic cells of the parabrachial region that project to the lateral geniculate nucleus (Bickford et al., 1993). NADPH-diaphorase staining suggests the presence of nitric oxide synthase (NOS) and thus that nitric oxide (NO) might also be used as a neurotransmitter by these cells. We sought to extend this light microscopic observation to the ultrastructural level by demonstrating the colocalization of NOS and choline acetyl transferase (ChAT; the synthetic enzyme for acetylcholine) in geniculate terminals.

Second, prior evidence (Jones and Powell, 1969b; Guillery, 1969a,b; de Lima et al., 1985; Cucchiari et al., 1988; Raczkowski and Fitzpatrick, 1989) suggests that both corticogeniculate and parabrachial axons form terminal endings of a very similar morphological type, the "RSD" terminal (see Materials and Methods for a further description of terminal types). RSD terminals make up roughly half the terminal population found in the lateral geniculate nucleus, and, although they are the dominant type found on peripheral dendrites, they also form many contacts on proximal dendrites (Guillery, 1969a, 1971; Wilson et al., 1984). However, in unstained material it has not been possible to identify which of these terminals is of cortical origin and which is of brainstem origin. It has also not been possible to determine the location of these inputs on the dendritic arbors of the targets. By labeling these terminals for additional study in a way that enabled us to determine their origin, we hoped to address these issues.

MATERIALS AND METHODS

We used brains from 11 adult cats for this study. Five of the cats were used for immunocytochemical study. They were given a fatal overdose of barbiturate and then perfused transcardially with a mixture of 4% paraformaldehyde and 0.2% glutaraldehyde. We extracted the brains, postfixed them in the same fixative for 2–8 hours, and cut them on a Vibratome at 50 μm in a sagittal plane. Finally, we collected the sections into phosphate-buffered saline (PBS; 1.8% NaCl in 0.01 M phosphate buffer). The other six cats were used for study of corticogeniculate terminals (see below).

Immunocytochemistry and histochemistry

BNOS. We selected sections through the lateral geniculate nucleus and brainstem. These were rinsed with PBS and preincubated in 0.03% Triton-X for 30 minutes. We found that such brief exposure to Triton-X was sufficient to improve the penetration of the antibody without causing so much tissue damage that the material became unsuitable for electron microscopy. We then reacted the sections with a 1:200 to 1:400 dilution of anti-BNOS (Transduction Laboratories, Lexington, KY) in PBS with 1% normal serum at 4°C for 2 days. After this, the sections were rinsed in PBS, transferred to a 1:100 dilution of biotinylated secondary antibody for 1 hour, rinsed in PBS, incubated in a mixture of 1:100 avidin and 1:100 biotinylated horseradish peroxidase (HRP) for 1 hour, rinsed in PBS, and visualized by a CoCl_2 -intensified 3,5-diaminobenzidine (DAB)-peroxidase reaction. We mounted some of these sections for light microscopy and prepared others for electron microscopy.

We selected some of the sections for double-labeling experiments to detect neural elements that stained positively for both BNOS and NADPH-diaphorase. To detect

both labels, we used a fluorescent tag for BNOS followed by standard NADPH-diaphorase histochemistry (see below). That is, we first performed the primary BNOS antibody incubation, rinsed the sections in PBS, incubated them in a 1:100 dilution of fluorescein avidin-D (Vector, Burlingame, CA) in PBS for 2 hours, and finally reacted them for NADPH-diaphorase.

ChAT. To reveal the light and electron microscopic localization of ChAT, we used a procedure similar to that described for BNOS. We used a 1:50 dilution of anti-ChAT (Boehringer-Mannheim, Indianapolis, IN) antibody as the primary. We also visualized this antibody with peroxidase or fluorescein as described above.

NADPH-diaphorase. We used a double-labeling protocol to reveal the colocalization of NADPH-diaphorase with antibodies raised against BNOS or ChAT. We incubated the sections with antibodies as described above and visualized them with fluorescein-tagged avidin. Then we rinsed the sections in Tris buffer and incubated them in a solution of 0.01% NADPH-diaphorase (Sigma, St. Louis, MO), 0.025 nitroblue tetrazolium, and 0.1 Triton-X in 0.5 M Tris buffered at pH 7.1 for 2–4 hours at 37°C. Finally, the sections were rinsed, mounted, air dried, briefly dehydrated, and coverslipped with Vectashield (Vector).

Labeling of corticogeniculate terminals

We placed an orthograde tracer (Biocytin-HCl; Sigma) into area 17, 18, or 19 in six cats to label corticogeniculate terminals.

Anesthesia and drugs. We first anesthetized the cats by an initial intravenous administration of 15 mg/kg pentobarbital (Nembutal). Additional doses of pentobarbital (2–5 mg/hour) and Acepromazine (1 mg/kg/hour) were given to maintain surgical anesthesia. We also infused physiological saline (5 ml/hour). A feedback-controlled heating blanket was used to maintain body temperature. All wound margins and pressure points were infused with Lidocaine to minimize pain and discomfort. The subjects appeared to remain deeply anesthetized throughout all phases of the cortical injections and surgery.

Surgery and tracer injections. Following the induction of anesthesia, each cat was placed in the stereotaxic apparatus, the skull was exposed, and a craniotomy was performed over the targeted visual cortical area. The borders of a target visual area were determined with the aid of cortical landmarks (Tusa et al., 1978, 1979). We targeted injections for regions mapping several degrees from the area centralis, and the labeling seen in the lateral geniculate nucleus occupied a retinotopic location consistent with this (Sanderson, 1971).

We used glass micropipette electrodes with 1.2 mm inner diameter for iontophoretic injection of the anterograde tracer biocytin (Biocytin-HCl; Sigma). The electrodes had tips that were broken to a diameter of 5 μm and filled with a 5% solution of biocytin in 0.9% NaCl. We iontophoresed with +1.5–5 μA constant current for 5–60 minutes. We targeted layer 6 for all injections, and subsequent histology confirmed success in this.

Histology. After a 12–36 hour survival period, each cat was given an overdose of sodium pentobarbital and perfused transcardially with 0.9% NaCl followed by a mixture of aldehydes (2% and 2% or 4% and 0.5% paraformaldehyde and glutaraldehyde, respectively) in 0.1 M phosphate buffer. We removed the brain and stored it in the perfusate for 6 hours. We then transferred it into phosphate buffer for 2 days at 4°C. The blocks containing

the lateral geniculate nuclei, the visual cortices, and the optic tracts were cut on a Vibratome. We processed serial sections for biocytin by pretreating them with 0.03% Triton X-100 for 30 minutes and incubating them in 1:100 avidin-biotinylated peroxidase complex in PBS overnight at 4°C. For some experiments, the Triton X-100 pretreatment was excluded. After several PBS rinses, the peroxidase was visualized by Ni or CoCl₂-intensified DAB reaction.

Electron microscopy

Two types of labeling were performed in association with electron microscopy, and these are described more fully in the following paragraphs. One, which we shall generally refer to as "preembedding," describes the labeling performed before embedding for electron microscopy. Preembedding label was visualized by horseradish peroxidase (HRP)-tagged secondary antibody. The other, which we refer to as "postembedding," describes the labeling performed after the embedding and visualized by gold-tagged secondary antibody.

Embedding. The geniculate sections that were reacted for biocytin, BNOS, or ChAT were trimmed to a selected area, placed in 2% osmium tetroxide (OsO₄) in 0.1 M PBS for 1 hour, and dehydrated in a graded series of ethyl alcohols. We transferred the sections first into a 1:1 mixture of resin (Durcupan ACM/Fluka; Electron Microscopy Sciences, Fort Washington, PA) and alcohol (100% ethyl alcohol), then into a 3:1 mixture of this resin and alcohol, and vacuum-infiltrated them in pure resin overnight. Sections were flat embedded between two pieces of Aclar (Ted Pella, Redding, CA) and a drop of resin and placed in a 68°C oven for 48–72 hours. We peeled the two pieces of Aclar away from the flat-embedded section and used a razor blade to block the area of interest on the section, which we then glued onto the end of a blank resin block. We cut thin sections at approximately 80 nm on an ultramicrotome. Each section was placed on one formvar-coated, nickel single slot grid. We counterstained every fifth or sixth thin section with uranyl acetate and lead citrate to add contrast.

Postembedding immunogold. We used a postembedding immunogold procedure to label profiles in a given section for either BNOS or γ -aminobutyric acid (GABA). The GABA labeling was used both to identify relay cells vs. interneurons (only the latter were GABA labeled) and also to help identify terminal types (see below). For postembedding immunocytochemistry, we followed a protocol modified from Phend et al. (1992). Briefly, thin sections were rinsed in Tris-buffered saline with Triton X (TBST) at pH 7.6 and incubated in a primary antibody in TBST at pH 7.6 for 24 hours. The primary antibody was either anti-GABA at 1:500 to 1:1,000 or anti-BNOS at 1:25 to 1:50. We then rinsed the sections first in TBST at pH 7.6 and then in TBST at pH 8.2. Following this, we incubated the sections in goat anti-rabbit IgG conjugated to gold particles (15 nm; Amersham Life Sciences, Arlington Heights, IL) at 1:25 in TBST at pH 8.2 for 1 hour. After this, the sections were rinsed in TBST at pH 7.6, followed by a rinse in deionized water, then placed in 2% glutaraldehyde (EM grade) for 10 minutes and counterstained as noted above.

We adopted a slight modification of our previously described method (Bickford et al., 1994) for distinguishing significant postembedding levels from background labeling. The control for background were terminals of retinal origin, known as "RLP" terminals (see below), because

these contain neither GABA nor BNOS, our two postembedding labels. We thus determined the frequency distribution of gold particle densities in all RLP terminals of each section studied. This distribution was determined separately for every thin section, because the overall amount of gold labeling varied among sections. We chose a 95% confidence level for the labeling: gold particle densities of all RLP profiles were ranked, and the 95th percentile reading was deemed the cutoff level for positive labeling for the given thin section.

Sampling of terminals. In general, the grids covered laminae A and A1, so both laminae were sampled, but no attempt was made to distinguish between them. When a terminal was seen with a synaptic contact, it was photographed and included in our sample. With the exception of labeled corticogeniculate terminals described below, terminals that did not display a clear synaptic contact in the section examined were ignored. From our unpublished results with serial reconstruction, we know that virtually all terminals in the geniculate neuropil form synapses, and we thus assume that those failing to show a synaptic contact in the present material would exhibit one in another section.

For terminals labeled with BNOS and/or ChAT, we examined the entire area of every sixth grid in a serial sequence. For anterogradely labeled corticogeniculate terminals, we scanned the entire extent of the projection column across the A-laminae. Because the biocytin injections in cortex were small, the columns of labeling in the A-laminae were roughly 600–800 μ m across. When we encountered a labeled terminal, we photographed it if it displayed a synaptic contact. Otherwise, we followed the labeled terminal through adjacent sections until the synaptic contact was reached, and we then photographed it. This was done to ensure that as many identified corticogeniculate terminals as possible were included in our sample.

Identification of terminal types

We used the morphological criteria based mainly on Guillery's (1969a,b) classification to evaluate synaptic profiles in the lateral geniculate nucleus. RLP terminals form asymmetrical contacts and have round vesicles, large profiles, and pale mitochondria (hence, RLP). These are known to be of retinal origin (Jones and Powell, 1969a; Rapisardi and Miles, 1984; Hamos et al., 1987). RSD terminals also form asymmetrical contacts and have round vesicles, small profiles, and dark mitochondria (hence, RSD). Most of these are thought to derive from cortex (Guillery, 1969a,b, 1971; Wilson et al., 1984; Montero, 1989; Weber et al., 1989), although some instead arise from brainstem (see below; see also de Lima et al., 1985; Cucchiari et al., 1988; Raczkowski and Fitzpatrick, 1989) or perhaps other sources (see, e.g., Van Horn et al., 1986). F terminals form symmetrical contacts and have flattened (hence, F) or pleomorphic vesicles. The great majority of these are thought to issue from local GABAergic neurons, either interneurons or cells of the nearby thalamic reticular nucleus. We identified a subset of these as F2 terminals (i.e., from dendritic appendages of interneurons) if they were vesicle filled and postsynaptic to any other terminal (Hamos et al., 1985). We also noted occasional profiles that had round vesicles and formed asymmetrical synapses but seemed too large to be typical RSD terminals and were clearly not RLP terminals. These may be a type recognized by others (Ide, 1982; Montero, 1989) in the perigeniculate

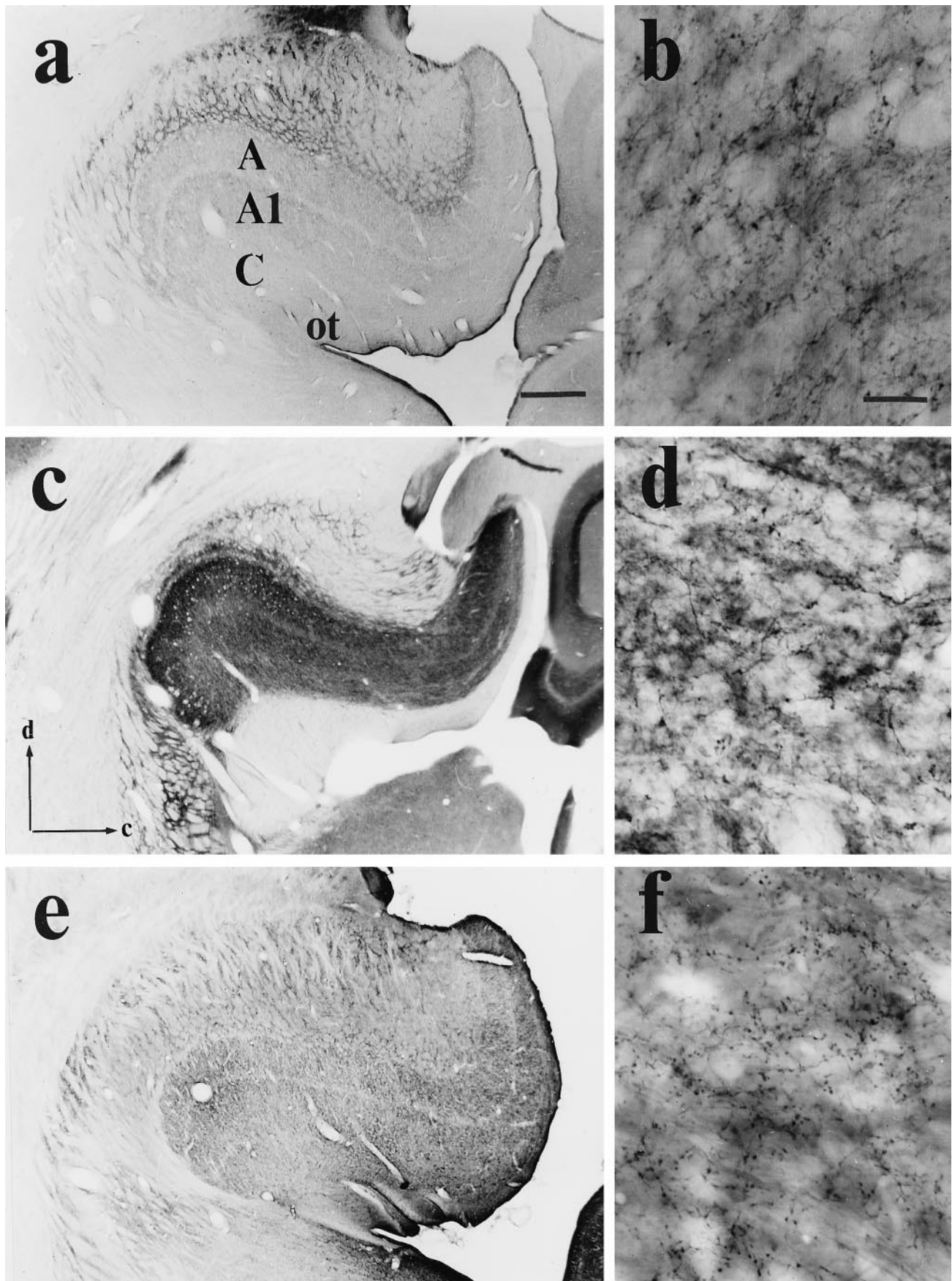


Fig. 1. Sagittal sections of the lateral geniculate nucleus. Lower (a) and higher (b) power views of staining with brain nitric oxide synthase (BNOS). Lower (c) and higher (d) power views of staining with NADPH-diaphorase. Lower (e) and higher (f) power views of

staining with choline acetyl transferase (ChAT). A, lamina A; A1, lamina A1; C, C-laminae; ot, optic tract; d, dorsal; c, caudal. Scale bar in a = 250 μ m (also applies to c, e); scale bar in b = 20 μ m (also applies to d, f).

nucleus as RLD (round vesicles, large profiles, and dark mitochondria). We clearly saw such terminals, albeit in small numbers, in the lateral geniculate nucleus (see below).

Identification of these types was generally straightforward for terminals without HRP reaction product in our biocytin-, BNOS-, or ChAT-stained sections. However, because of the processing and staining protocols we used to obtain the HRP label, identification of vesicle shape was compromised for the terminals so labeled. RLP terminals were always clearly recognized, because their large size and pale mitochondria make them readily identifiable even when labeled (cf. Hamos et al., 1987). None of the RLP terminals in our material was labeled by biocytin, BNOS, or ChAT. However, the limitation imposed by the HRP reaction product meant that, without further data, we could not in some cases distinguish F terminals from RSD (or RLD) terminals among the subset of labeled terminals. This problem was partly solved with the post-embedding GABA labeling described above: Any GABA⁺ terminal was deemed to be an F terminal, and any terminal that was not an RLP terminal and was GABA⁻ was deemed to be an RSD (or RLD) terminal.

RESULTS

We had previously demonstrated that, in the cat, the cholinergic cells of the brainstem parabrachial region that innervate the lateral geniculate nucleus also stain positively by NADPH-diaphorase histochemistry (Bickford et al., 1993). This enzymatic reaction is thought to indicate the presence of NOS, suggesting that these parabrachial neurons may use both acetylcholine (ACh) and NO as neurotransmitters. We performed further studies to extend these observations. First, at the light microscopic level, we demonstrated that an antibody directed against BNOS stains fibers and puncta within the lateral geniculate nucleus whose morphology is identical to the morphology of those stained with either NADPH-diaphorase or ChAT. Second, we demonstrated that BNOS stains the same cells in the parabrachial region that stain positively for NADPH-diaphorase. Third, with the electron microscope, we demonstrated that the vast majority of cholinergic terminals within the lateral geniculate nucleus also contain BNOS. Fourth, we compared the morphological features of corticogeniculate and parabrachial terminals. These studies are discussed in detail below.

Staining of parabrachial cells and fibers: Light microscopy

Fiber staining in the lateral geniculate nucleus.

Figure 1 shows the close similarity in the staining patterns of BNOS, NADPH-diaphorase, and ChAT in the neuropil of the lateral geniculate nucleus. Three similar sections are illustrated, each stained for one of the above-mentioned markers. Figure 1a,b shows a lower and higher power view of the staining for BNOS, Figure 1c,d does this for NADPH-diaphorase, and Figure 1e,f does this for ChAT. The higher power views are within matched regions of lamina A.

Note that the staining for all three substances is quite similar. It is limited to fibers and puncta, the latter presumably representing synaptic terminals (see below), and no somata are detectably labeled in the A-laminae (Fig. 1b,d,f; but see below). The staining in the thalamic reticular nucleus (including the perigeniculate nucleus) is darker than that in the A-laminae, and the staining in the

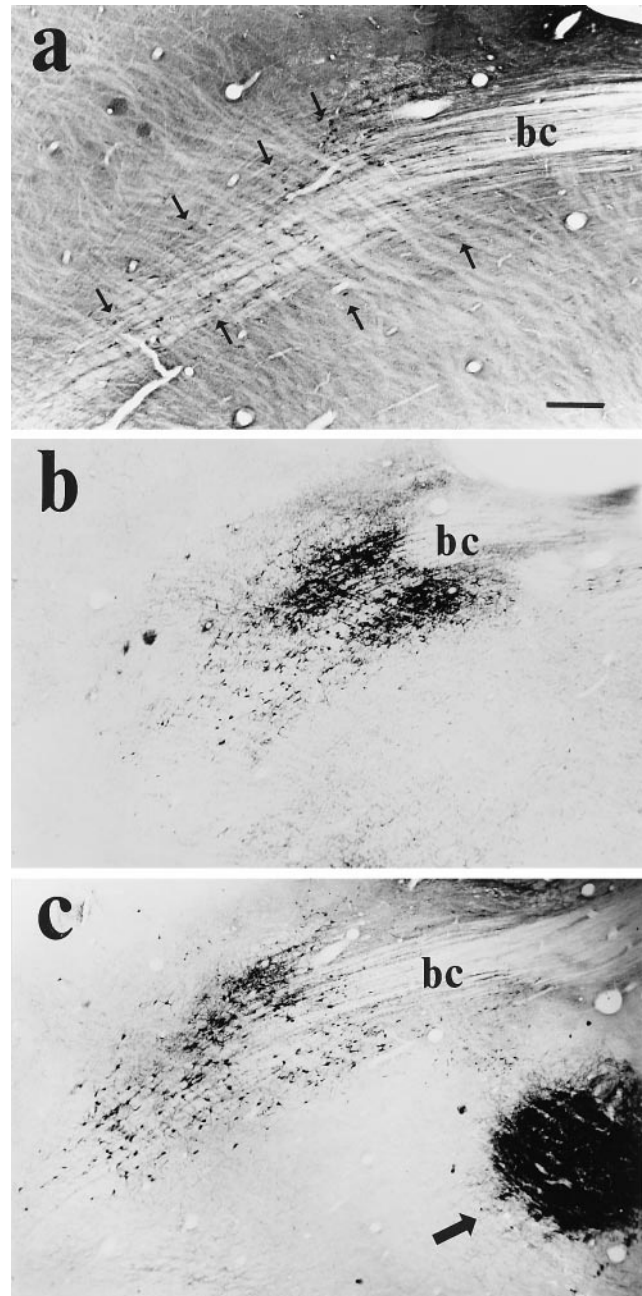


Fig. 2. Sagittal sections of the brainstem parabrachial region in the cat in the region of the brachium conjunctivum (bc). **a:** Staining with BNOS. Because this staining has more background labeling, the labeled cells are difficult to see at this magnification. Arrows point to labeled cells to help identify them. **b:** Staining with NADPH-diaphorase. **c:** Staining with ChAT. Note that the trochlear nucleus (arrow) is stained positively for ChAT, because it contains cholinergic oculomotor neurons. Note also that, in the comparable location of the trochlear nerve, there is no staining for BNOS (a) or NADPH-diaphorase (b). Thus, BNOS and NADPH-diaphorase staining are not a common property of all cholinergic cells. Scale bar = 250 μ m.

A-laminae, in turn, is somewhat darker than that in interlaminar regions and the C-laminae (Fig. 1a,c,e).

Cell staining in the parabrachial region. We have shown previously that the sole source of fibers and puncta

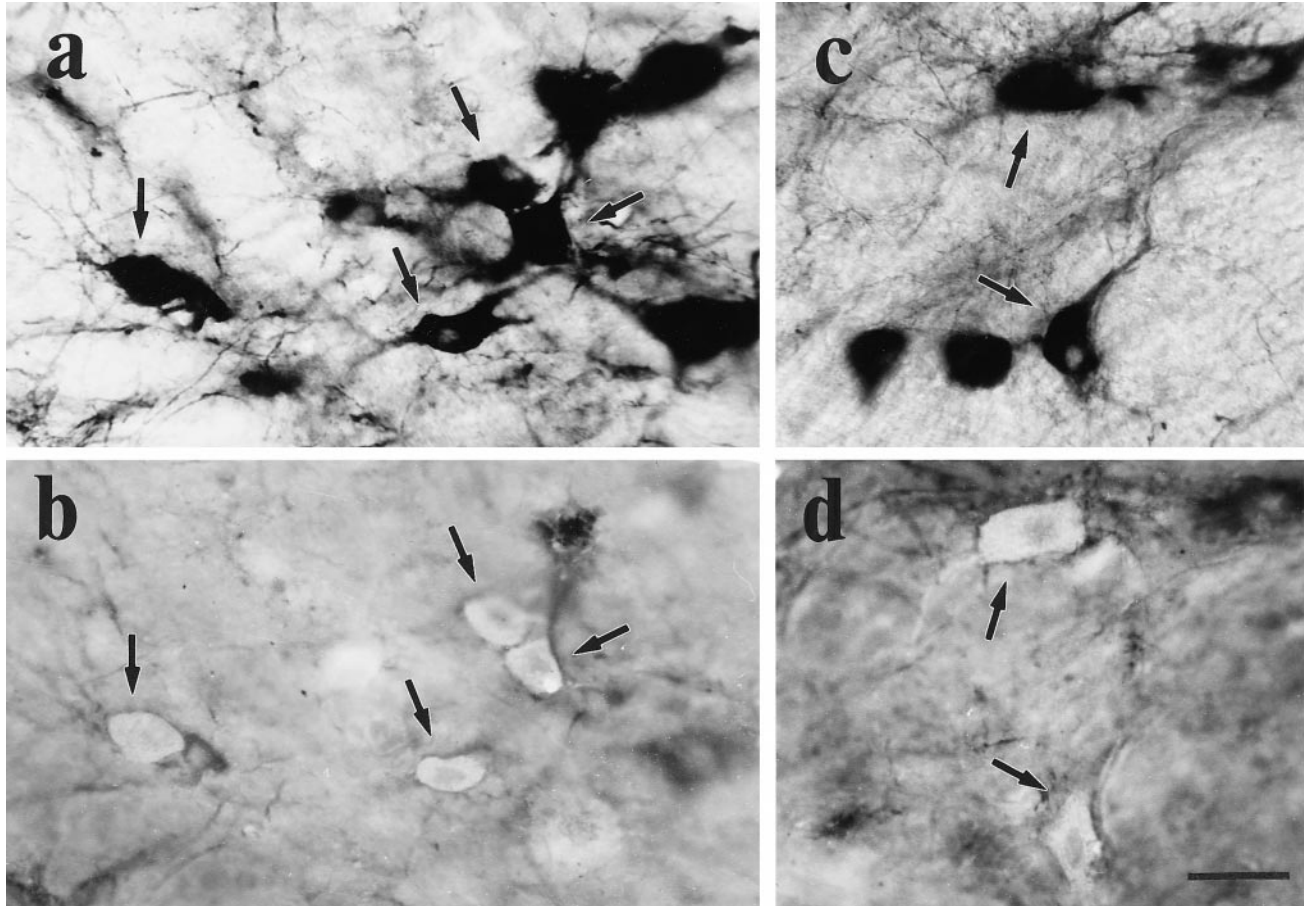


Fig. 3. Double labeling of parabrachial cells with NADPH-diaphorase (a, c) and BNOS (b, d). Arrows point to representative double-labeled cells in the same sections (a and b, c and d). Scale bar = 10 μ m.

in the lateral geniculate nucleus staining positively for NADPH-diaphorase (see Fig. 1c–f) is the cholinergic cell population of the parabrachial region (Bickford et al., 1993). Figure 2 presents a lower power view of the analogous staining of the parabrachial region, showing positive reactions for BNOS (Fig. 2a), NADPH-diaphorase (Fig. 2b), and ChAT (Fig. 2c). The NADPH-diaphorase and ChAT staining labels both somata and neuropil, so it is easily seen at lower power. The BNOS labeling, however, is essentially limited to somata, and this is difficult to see at lower power (but see below). Thus, arrows are shown in Figure 2a to indicate somata labeled for BNOS. The patterns of somata labeled by the three substances are remarkably similar.

Double labeling of parabrachial cells with BNOS and NADPH-diaphorase. To determine whether the BNOS antibody is specific to the parabrachial cells that stain positively for NADPH-diaphorase, we used double-labeling techniques. We visualized the BNOS label on sections through the parabrachial region with a fluorescein-tagged secondary antibody and then reacted the same sections for NADPH-diaphorase. Figure 3a,c shows two higher power views of the parabrachial region in transmitted light. Many cells darkly stained for NADPH-diaphorase are evident. Figure 3b,d shows the identical fields of view with epifluorescent illumination, and the cells contain-

ing BNOS are now illuminated. The arrows in each panel indicate double-labeled cells.

Figure 4 shows a plot of parabrachial cells stained for NADPH-diaphorase and/or BNOS. Plots for two different sections from two animals are shown. The cells single labeled for NADPH-diaphorase are indicated by open circles, those single labeled for BNOS are indicated by crosses, and those double labeled for NADPH-diaphorase and BNOS are indicated by solid circles. Nearly all of the cells positive for BNOS were also stained by NADPH-diaphorase. In fact, every one of the 105 cells positive for BNOS was double labeled in one section (Fig. 4a), and 86 of 92 (93%) such cells were double labeled in the other (Fig. 4b). Overall, 191 of 197 (97%) cells positive for BNOS were double labeled. Many more cells were singly labeled for NADPH-diaphorase, 136 in Figure 4a and 199 in Figure 4b. However, because the staining for NADPH-diaphorase involves a histochemical reaction that exposes every neuron, whereas the BNOS labeling involves immunocytochemistry that limits exposure of neurons to the antibody because of penetration limitations, it is likely that many of the cells singly labeled for NADPH-diaphorase also contain BNOS that went undetected. In any case, we can conclude that virtually every parabrachial cell containing BNOS also stains positively for NADPH-diaphorase.

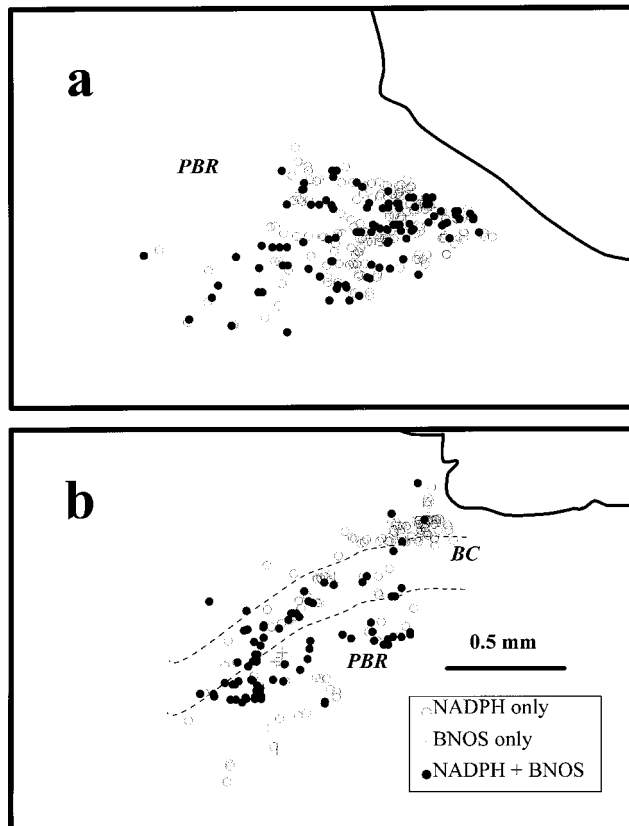


Fig. 4. Distribution of cells in the parabrachial region (PBR) labeled for NADPH-diaphorase and/or BNOS. One section each is shown from a different animal in sagittal view. The outline of the brachium conjunctivum (BC; dashed lines) is shown in **b**; the view in **a** is more lateral, and the brachium conjunctivum is no longer clearly present. Note that nearly all of the cells labeled for BNOS also stain positively for NADPH-diaphorase. Although there are many more cells labeled singly for NADPH-diaphorase than for BNOS, this probably reflects the limited penetration of the BNOS antibody, a limitation not applicable to NADPH-diaphorase staining.

Staining of parabrachial profiles: Electron microscopy

Our light microscopic observations indicate that the cells in the parabrachial region that innervate the lateral geniculate nucleus contain the synthesizing enzymes for both ACh and NO and that the patterns of fiber staining in the geniculate neuropil are very similar for NADPH-diaphorase, ChAT, and BNOS labels (see above; see also Bickford et al., 1993). To determine with greater resolution the pattern of BNOS labeling in these sections, we used the electron microscope to examine thin sections through the geniculate A-laminae and photographed the regions containing the label. We found that most BNOS-labeled profiles were synaptic terminals, but some were dendrites. For each labeled terminal, we determined whether it contained vesicles, its morphological type (see Materials and Methods), its location presynaptic or postsynaptic to another profile, and its location within or outside of an encapsulated glomerular zone. We also determined the nature of terminals forming nearby synapses onto any profile postsynaptic to the labeled terminal under study.

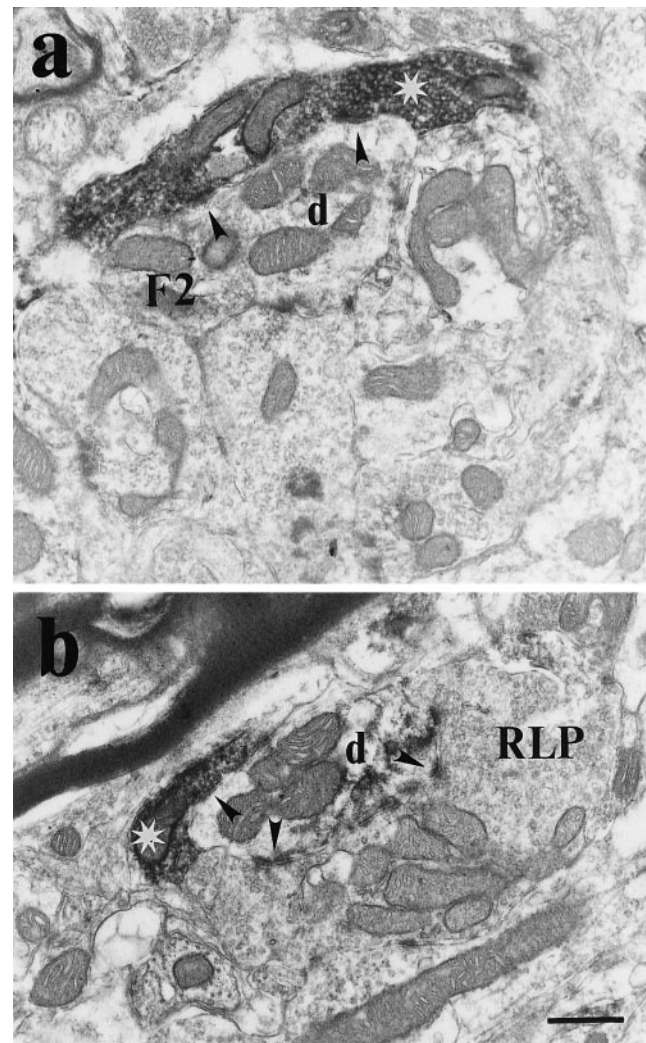


Fig. 5. Terminals labeled for BNOS in the geniculate A-laminae. The asterisks mark labeled terminals, and arrowheads indicate synaptic contacts from these labeled terminals onto dendrites (d). **a**: Labeled terminal located peripherally within a glomerulus, which also contains an RLP terminal (not illustrated) and an F2 terminal. **b**: Labeled terminals located outside a glomerulus near an RLP terminal (RLP) contacting the same dendrite (synapse not shown). The terminal labeled for BNOS shows typical RSD morphology. Scale bar = 500 nm.

Morphological characteristics of BNOS-labeled terminals. BNOS-labeled terminals varied in size and shape, had mostly round vesicles and dark mitochondria, and formed asymmetrical synapses. They were also unlabeled for GABA (see also below). Most terminals labeled for BNOS resembled RSD terminals as initially described by Guillery (1969b). However, some of the BNOS-labeled terminals seemed too large to be typical RSD terminals (see also below) and instead displayed RLD morphology. Figures 5 and 6 illustrate typical examples of terminals in the A-laminae that stain positively for BNOS. They were found both inside and outside of glomeruli, and they formed synapses mostly onto dendrites (Figs. 5a,b, 6a) but also onto vesicle-filled profiles (Fig. 6b). The only postsynaptic vesicle-filled profiles in the geniculate circuitry are dendritic appendages of the interneurons, which were

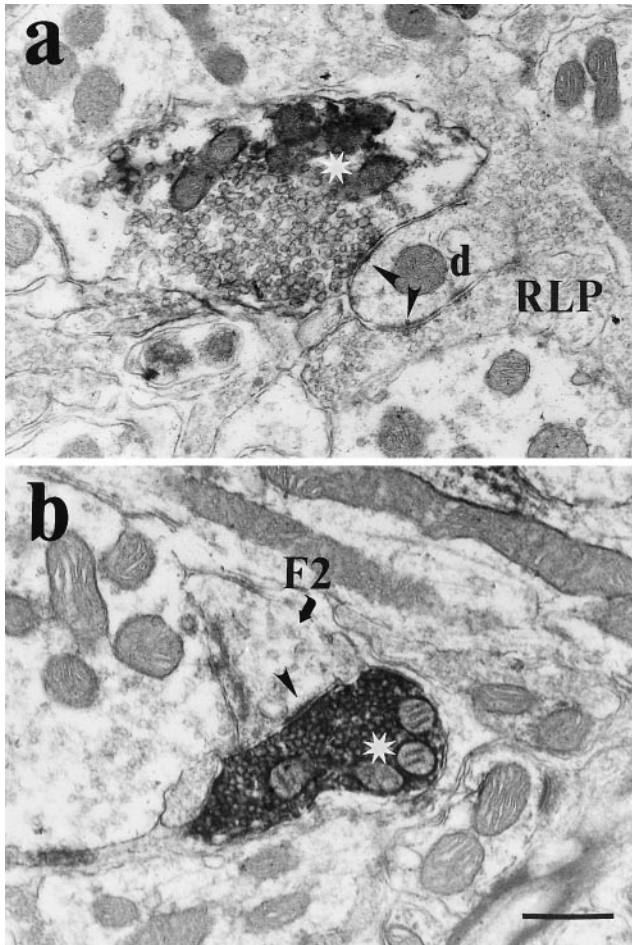


Fig. 6. Terminals labeled for BNOS (asterisks) in the geniculate A-laminae; notations and abbreviations as in Figure 5. **a:** Labeled terminal with RLD morphology contacting dendrite. **b:** Labeled terminal contacting F2 profile (F2). Scale bar = 500 nm.

previously described as F2 terminals (Hamos et al., 1985). Therefore, such targets of the BNOS-positive terminals are labeled accordingly.

Evidence that BNOS is contained in dendrites of interneurons. Although most of the BNOS label we encountered was in terminals, occasionally we saw light BNOS labeling in dendritic profiles. Figure 7a shows an example of such dendritic labeling. To determine whether these dendrites are from relay cells or interneurons, we used the double-labeling protocol for both BNOS and GABA as described in Materials and Methods. Figure 7a,b shows the result of such double labeling. Note that the BNOS-labeled terminal does not have significant GABA labeling but that the BNOS-labeled dendrite does.

To identify the dendritic profiles double labeled for BNOS and GABA, we photographed the grids processed for both the preembedding BNOS label and the postembedding GABA label. We calculated the 95% confidence level for background gold density as described in Materials and Methods and adopted this value as the criterion density for GABA labeling in each grid. The ratio of labeling to this cutoff level was then computed for profiles labeled for BNOS. Figure 8 shows the results of these double-labeling

studies. None of the 41 labeled terminals expressed GABA labeling gold densities that exceeded background levels (Fig. 8a). In contrast, 14 of 16 (88%) dendrites containing the BNOS label also stained for GABA. We conclude that the vast majority of dendrites containing BNOS also contain GABA and thus represent dendrites of interneurons. Interestingly, although this indicates that at least some interneurons contain BNOS in their dendrites, we did not see such labeling in any somata, and this confirms our observations with the light microscope (see Fig. 1).

Terminals labeled for ChAT. Figure 1 shows great similarity in the fiber and terminal staining patterns for NADPH-diaphorase, BNOS, and ChAT within the lateral geniculate nucleus. Prior evidence indicates that much of this staining emanates from parabrachial cells that contain both ChAT and BNOS (see above; see also Bickford et al., 1993), which in turn suggests that the terminals labeled with BNOS in the A-laminae might also contain ChAT. Figure 9 shows an example of a ChAT-labeled terminal. As with the terminals labeled for BNOS, the ChAT-labeled terminals were found both in glomerular and in extraglomerular zones (see also below; see also Raczkowski and Fitzpatrick, 1989). The terminals labeled for ChAT bore many features of RSD terminals, except that some were large enough to be RLD terminals (see also below).

Evidence that cholinergic terminals contain BNOS. The observations described above strongly indicate that terminals labeled for BNOS share many morphological features with those labeled for ChAT. To test the hypothesis in a more convincing manner that terminals labeled for BNOS and ChAT actually represent the same terminal population, we performed double-labeling studies to identify any terminals containing both BNOS and ChAT.

To identify terminals double labeled with BNOS and ChAT, we used an approach basically similar to that described above for dendritic profiles double labeled for BNOS and GABA, except we used an immunogold procedure to label BNOS instead of GABA. RLP terminals still served as the control for background labeling. Figure 10a shows a typical example of a terminal labeled preembedding with ChAT and then double labeled postembedding with BNOS. Figure 10b shows a tracing of the main elements in the photograph in Figure 10a, with the gold particles conspicuously indicated. The ChAT-labeled profile clearly has a higher density of gold particles than does the surrounding neuropil. Figure 11 shows the normalized BNOS labeling density in our population of 74 terminals labeled for ChAT. Every one of these terminals had a higher-than-background density of BNOS label. We thus conclude that all terminals labeled for ChAT also contain BNOS.

Because all of the ChAT-labeled terminals also contained BNOS, we assumed for further analyses described below that all terminals labeled preembedding for either BNOS or ChAT represent the same terminal population. We have previously shown that these terminals derive from the parabrachial region (Bickford et al., 1993). We shall therefore refer to these terminals labeled by BNOS and/or ChAT as parabrachial terminals.

Pattern of synaptic contacts made by parabrachial terminals onto relay cells. Previous studies of the pattern of synaptic input onto relay cells in the geniculate A-laminae indicate that two general zones can be defined

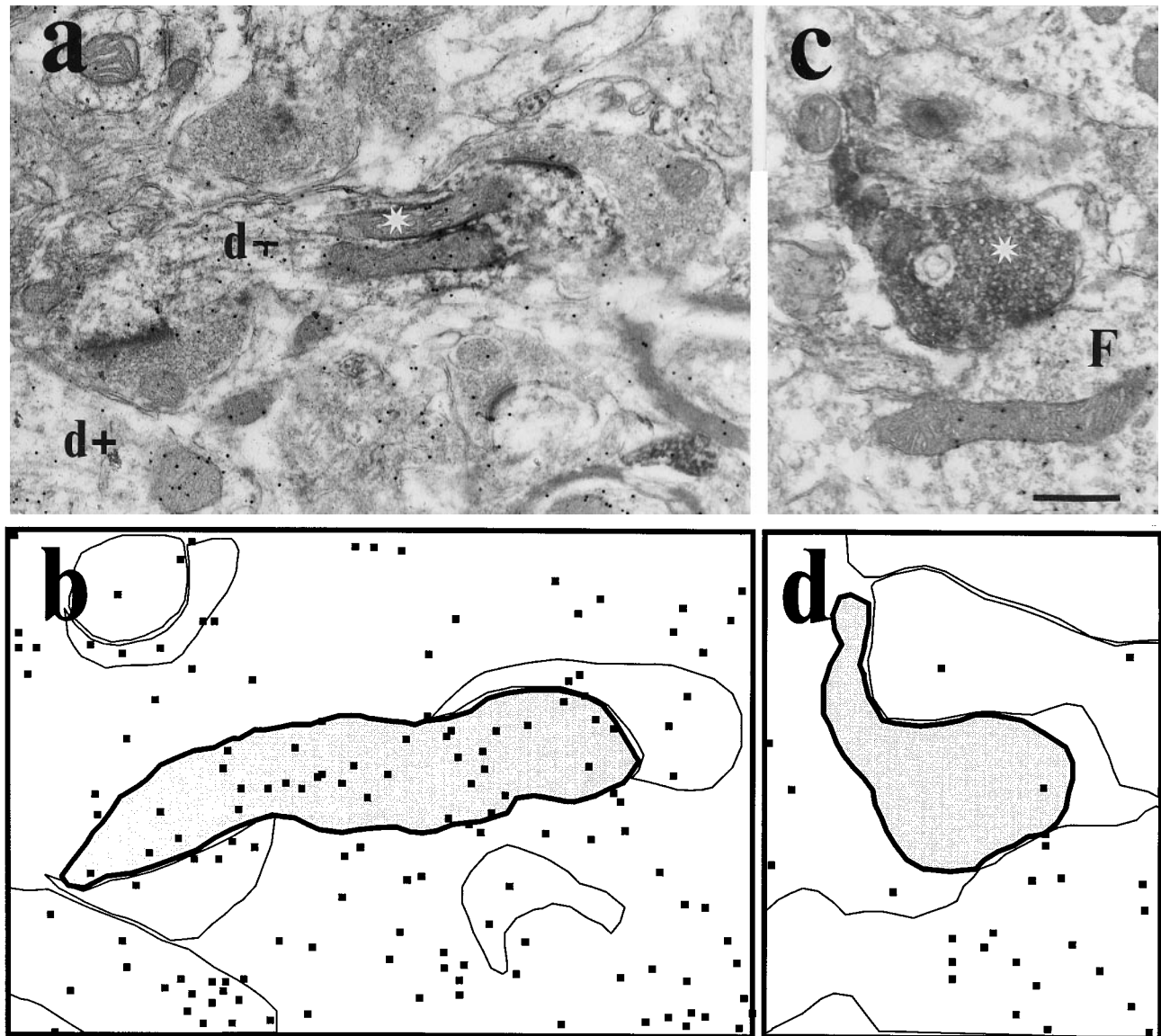


Fig. 7. Double labeling of profiles for BNOS and GABA. Labeling as in Figure 5. The BNOS labelling is done before embedding and is the label tagged with horseradish peroxidase (HRP), whereas the GABA is labeled postembedding and tagged with gold particles. **a:** Labeling for BNOS (asterisk) and GABA (d+) in dendrites. One dendrite in the middle of the panel includes both labels; another, at the lower left, is labeled only for GABA. **b:** Line drawing of **a** with the gold

particles shown as squares and the BNOS labeled profile shaded. This is shown, because from photographs such as that in **a** reproduced for publication, it is often difficult to detect the gold particles amidst the HRP tag. Note the relatively dense GABA labeling in the dendrite labeled for BNOS. **c:** Terminal labeled for BNOS (asterisk) but not GABA. An F terminal (F) is seen labeled for GABA but not BNOS. **d:** Line drawing of **c**. Scale bar = 500 nm.

with respect to the dendritic arbors of these postsynaptic cells: Their proximal dendrites are the site of retinal inputs, although other terminal types also contact these cells proximally, and their distal dendrites are the site of virtually all cortical inputs, and very few other terminals (occasional F terminals, but no RLP or RLD terminals) contact these distal dendrites (Wilson et al., 1984; Cucchiari et al., 1991b). Thus, the *retinal recipient zone* lies proximally and is characterized by the presence of synaptic contacts from RLP terminals. Glomeruli are almost all found proximally and would thus be associated with the retinal recipient zone (Szentágothai et al., 1966; Jones and Powell, 1969a; Wilson et al., 1984; Hamos et al., 1987). The

cortical recipient zone lies distally and is characterized by extraglomerular synapses and the presence of RSD terminals, which is the terminal type found on cortical axons (Guillery, 1969a,b, 1971; Montero, 1989; Weber et al., 1989; Wilson et al., 1984; see also below). If enough of the postsynaptic dendritic profile can be viewed with the electron microscope, which was the case for most of our observations of relay cells, it is possible to identify these zones.

When we could clearly identify the postsynaptic region of a relay cell contacted by parabrachial terminals, this was *always* in a retinal recipient zone. In these cases, profiles postsynaptic to parabrachial terminals were inner-

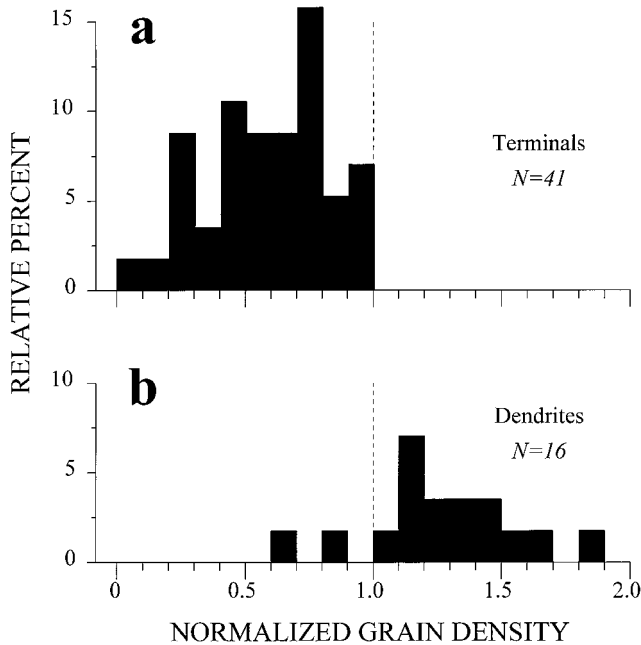


Fig. 8. Distribution of profiles double labeled for BNOS tagged with HRP before embedding and GABA tagged with gold particles after embedding. The dashed lines represent the level of background GABA labeling based on density of gold particles in RLP terminals. **a**: BNOS-labeled terminals. None of these terminals had a GABA labeling level more than background. **b**: BNOS-labeled dendrites. Most of these expressed GABA labeling that was above background.

vated as well by RLP terminals. Figure 5 shows examples of this. Some parabrachial terminals were found within glomeruli and others outside of glomeruli (see also below). The labeled terminal shown in Figure 5a is located within a glomerulus. Figure 5b shows a labeled terminal in an extraglomerular region, and the postsynaptic dendrite is also contacted in the same region by an RLP terminal. When we found a labeled terminal contacting a postsynaptic profile in the retinal recipient zone, we never saw unlabeled RSD terminals contacting the same profile. Parabrachial terminals thus contacted geniculate neurons in a highly specific fashion that suggests the possibility that they selectively affect retinogeniculate transmission.

From the above-described observations, it seems clear that some parabrachial terminals are found inside glomeruli and others outside. In our material, we could not always confidently determine whether a terminal location was glomerular, but we could do so for 85 of the 123 terminals labeled for BNOS and/or ChAT. Of these, 34 were found inside glomeruli and 51 were found outside. However, we found no discernible morphological differences to correlate with their glomerular involvement.

Comparison of parabrachial, corticogeniculate, and RSD terminals

RSD terminals represent the largest terminal population found in the A-laminae, and the two best known contributors to this population are corticogeniculate terminals (Jones and Powell, 1969b; Montero, 1989; Weber et al., 1989) and terminals from the brainstem parabrachial region (de Lima and Singer, 1987b; Cucchiari et al., 1988;

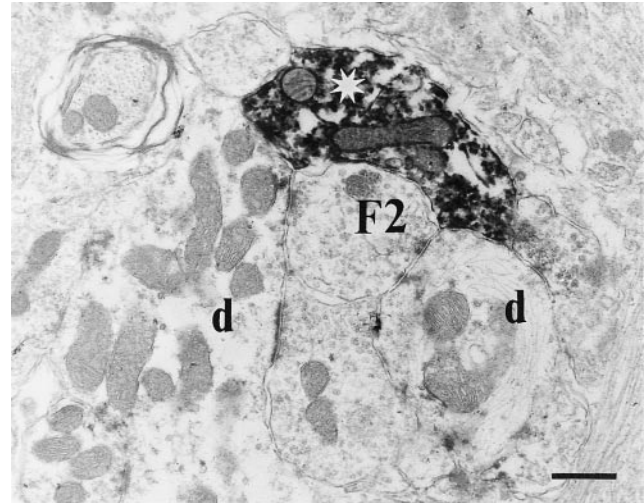


Fig. 9. Terminals labeled for ChAT (asterisk) in the geniculate A-laminae; notations and abbreviations as in Figure 5. Scale bar = 500 nm.

Raczkowski and Fitzpatrick, 1989). We sought to compare these two terminal populations. We could identify parabrachial terminals by ChAT or BNOS labeling and corticogeniculate terminals by orthograde transport of biocytin injected into area 17, 18, or 19. We also compared these histochemically identified terminals to morphologically identified RSD terminal population within the same sections.

Size differences of parabrachial, cortical, and RSD terminals. As noted above, the morphological characteristics of parabrachial terminals resembled those of the RSD terminals, except for some that were large enough to be RLD terminals. This is consistent with the earlier observation that terminals labeled for ChAT (i.e., the parabrachial terminals) are larger than unlabeled RSD terminals (Raczkowski and Fitzpatrick, 1989), but RLD terminals were evidently not considered in this earlier study. To investigate this further, we compared the sizes of parabrachial terminals with unlabeled RSD and RLD terminals. Figure 12a shows the distribution of 183 of these terminals found in sections unlabeled for any marker, and Figure 12b shows the size distribution for 115 parabrachial terminals. Note that, even with the addition of RLD terminals to RSD terminals, the identified parabrachial terminals are still, on average, significantly larger ($0.52 \pm 0.32 \mu\text{m}^2$ for Fig. 12a vs. $0.77 \pm 0.43 \mu\text{m}^2$ for Fig. 12b; $P < 0.001$ on a Mann-Whitney U test), but also note that the range of sizes is roughly the same for both distributions. This last point suggests that many if not all RLD terminals derive from the brainstem.

Because corticogeniculate terminals also have RSD morphology and thus share this feature with many parabrachial terminals, we compared the sizes of these populations. Figure 12c shows the size distribution of 437 corticogeniculate terminals labeled from injection of biocytin into visual cortex (see Materials and Methods). The cortical terminals ($0.36 \pm 0.14 \mu\text{m}^2$) were significantly smaller than both the unlabeled RSD plus RLD terminals and the labeled parabrachial terminals ($P < 0.001$ on a Mann-Whitney U test for both comparisons).

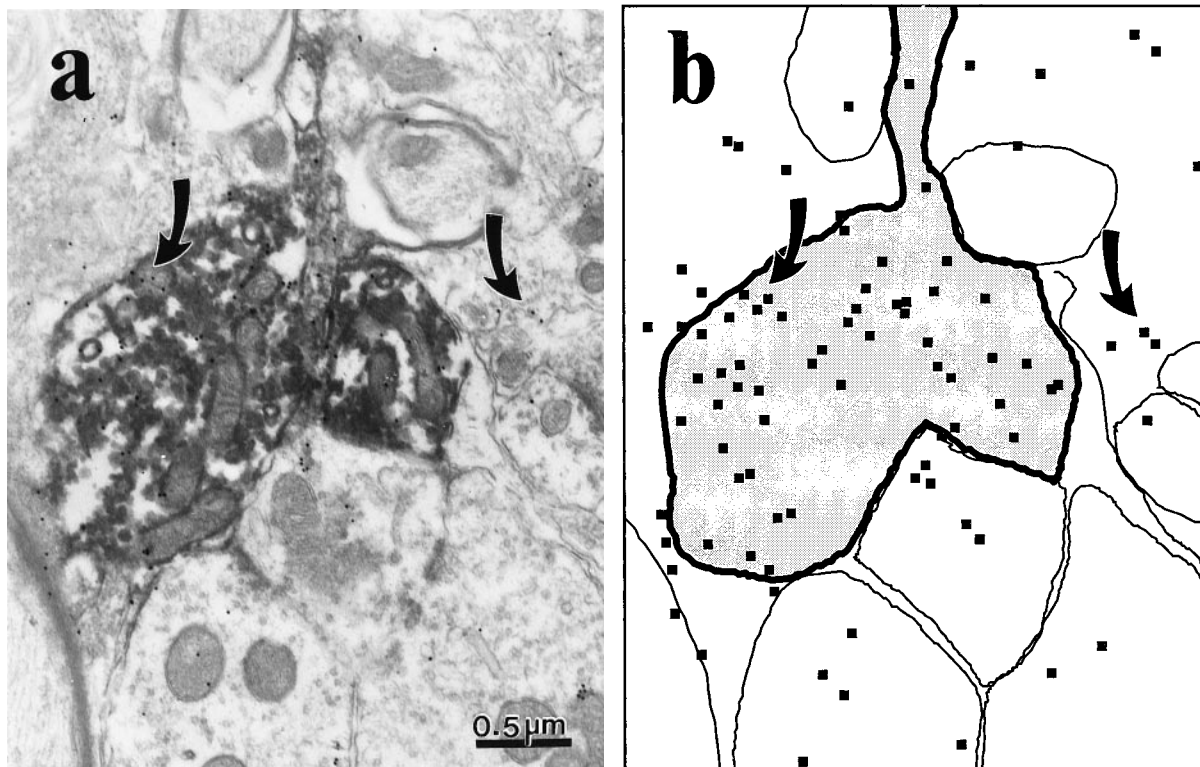


Fig. 10. Double labeling of a terminal in the geniculate A-laminae for ChAT and BNOS. The ChAT labeling is done before embedding and the label is tagged with HRP, whereas the BNOS is labeled postembedding and tagged with gold particles. **a:** Electron micrograph of

double-labeled terminal. **b:** Line drawing as in Figure 7. The higher density of BNOS labeling in the terminal labeled for ChAT is readily evident. The arrows in a and b point to the same areas in each panel.

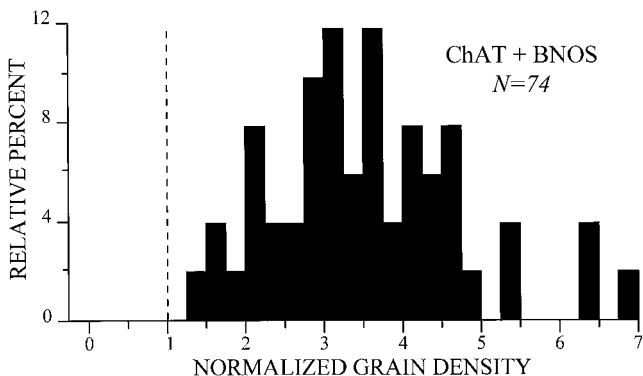


Fig. 11. Distribution of terminals double labeled for ChAT tagged with HRP before embedding and BNOS tagged with gold particles after embedding. The dashed line represents the level of background BNOS labeling based on density of gold particles in RLP terminals. Every one of the terminals labeled for ChAT had a BNOS labeling level above background.

Relative location of corticogeniculate and parabrachial terminals. As noted above, the parabrachial terminals identified via their BNOS and/or ChAT staining terminated exclusively or nearly so in the retinal recipient zone of geniculate neurons. In contrast, *none* of the labeled corticogeniculate terminals on relay cells was found in a retinal recipient zone of a relay dendritic arbor; further-

more, *none* of the 437 labeled corticogeniculate terminals was found within a glomerulus. The termination zones of corticogeniculate and parabrachial terminals are thus quite distinct on relay cells.

DISCUSSION

These experiments provide further information on the nature of the input from the parabrachial region of the brainstem to the lateral geniculate nucleus and its relationship to the corticogeniculate input. Together, these pathways represent the vast majority of the excitatory, nonretinal input to this thalamic relay nucleus. They thus play a major role in controlling the flow of retinal information to cortex.

Staining for BNOS in the lateral geniculate nucleus

Parabrachial terminals. In prior experiments, we have shown that the cholinergic cells of the brainstem parabrachial region that innervate the lateral geniculate nucleus stain positively for NADPH-diaphorase (Bickford et al., 1993). We have also demonstrated that these cholinergic parabrachial cells are the only cells that project to the lateral geniculate nucleus and stain positively for NADPH-diaphorase (Bickford et al., 1993). NADPH-diaphorase staining is associated with the presence of NOS, which suggests that this parabrachial innervation to

the lateral geniculate nucleus uses both ACh and NO as neurotransmitters or neuromodulators.

In the present study, we have extended this in several ways. First, we have shown that staining for an antibody directed against BNOS exhibits the same pattern of labeling as does the NADPH-diaphorase reaction. This is true both for the pattern of axons and puncta staining in the lateral geniculate nucleus as well as for soma staining among parabrachial neurons. Second, we have shown that terminals in the lateral geniculate nucleus that label for ChAT also label for BNOS, and we can conclude that these derive from parabrachial axons. These new data point more strongly to the conclusion that the parabrachial input to the lateral geniculate nucleus uses both ACh and NO to influence the relay of retinal information to cortex.

Ample evidence exists that parabrachial activation can strongly influence the nature of the relay of retinal information through the lateral geniculate nucleus (Lu et al., 1993; Hartveit and Heggelund, 1995; Uhlrich et al., 1995). What is less clear is precisely how these effects relate to release of ACh and NO. More is known about the effects of ACh application onto relay cells, and this not only excites them but also changes their mode of response from burst to tonic firing based mainly on the inactivation of a voltage-dependent Ca^{2+} conductance (Jahnsen and Llinás, 1984a,b; McCormick, 1992), and this is also seen with parabrachial activation in vivo (Lu et al., 1993). Fewer studies have been directed at effects of NO on relay cell responses, but there is evidence that such effects exist (Pape and Mager, 1992; Cudeiro et al., 1994a,b, 1996). One of the effects seen, which is based on in vivo recording, is that NO release, presumably from parabrachial terminals, is necessary for retinal inputs to activate N-methyl-D-aspartate (NMDA) receptors on geniculate relay cells (Cudeiro et al., 1994a,b, 1996).

This is interesting because an analogous effect is claimed for the hippocampus. In hippocampus, however, NO is thought to be released from the postsynaptic pyramidal cells on activation of certain synapses to amplify transmission of these synapses, and long-term potentiation may involve such a process involving NO release from the postsynaptic site (Madison, 1993; Schuman and Madison, 1994; Dinerman et al., 1994). NO release from parabrachial terminals may provide a similar function, but here it is controlled from the parabrachial region and not from the relay cells themselves. Key to this is the proximity of parabrachial and retinal terminals on the relay cell dendrites. This offers another way in which parabrachial inputs can affect the retinal relay through the lateral geniculate nucleus. Also, recent evidence suggests possible links between muscarinic receptors and NO activity (Wang et al., 1994; Mathes and Thompson, 1996). Whatever the function of NO release, our data suggest that parabrachial terminals release NO and ACh conjointly, and, to understand better the function of parabrachial inputs, it may be important to study the effects of conjoint application of ACh and NO.

Interneurons. The only postsynaptic sites of BNOS we found were dendrites of interneurons. From our material, it is unclear how many interneurons contain BNOS, but at least a subset does. Presumably any BNOS present in the somata of these interneurons was at a level too low to detect with our techniques. As was noted in the preceding paragraph, the postsynaptic presence of NO has been

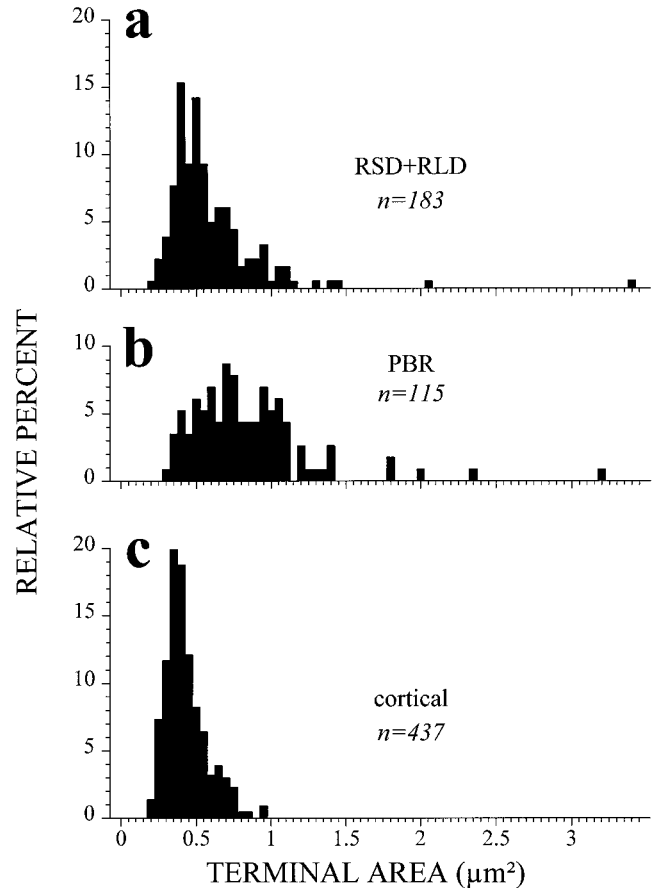


Fig. 12. Size distributions of three different populations of terminals seen in the A-laminae of the cat's lateral geniculate nucleus. The sizes are based on cross-sectional areas. See text for further definitions of these terminal types. **a:** RSD plus RLD terminals from sections in which no staining for biocytin, BNOS, or ChAT was done. **b:** Terminals from the parabrachial region (PBR), identified by labeling with BNOS and/or ChAT. **c:** Corticogeniculate terminals (cortical) labeled by anterograde transport of biocytin injected into cortical area 17, 18, or 19.

suggested for hippocampal pyramidal cells, and this may be involved in controlling efficacy of certain inputs to these cells. Whether any such mechanism exists in the lateral geniculate nucleus is unknown, but the pattern of BNOS labeling we have seen suggests that such mechanisms would be limited to interneurons.

Relationship between corticogeniculate and parabrachial terminals

Terminal morphology. Nonretinal terminals that form asymmetric synapses in the lateral geniculate nucleus may be considered as a broad class subsumed under the heading of "RSD," although a few rare representatives are too large to be typical RSD terminals. For want of a better term, we have referred to these as "RLD." We could not, in unstained material, see evidence for several classes subsumed within this "RSD plus RLD" population in terms of size and other features we observed, because this seemed to be a unimodal grouping with no clear division between RSD and RLD terminals. However, once we applied other

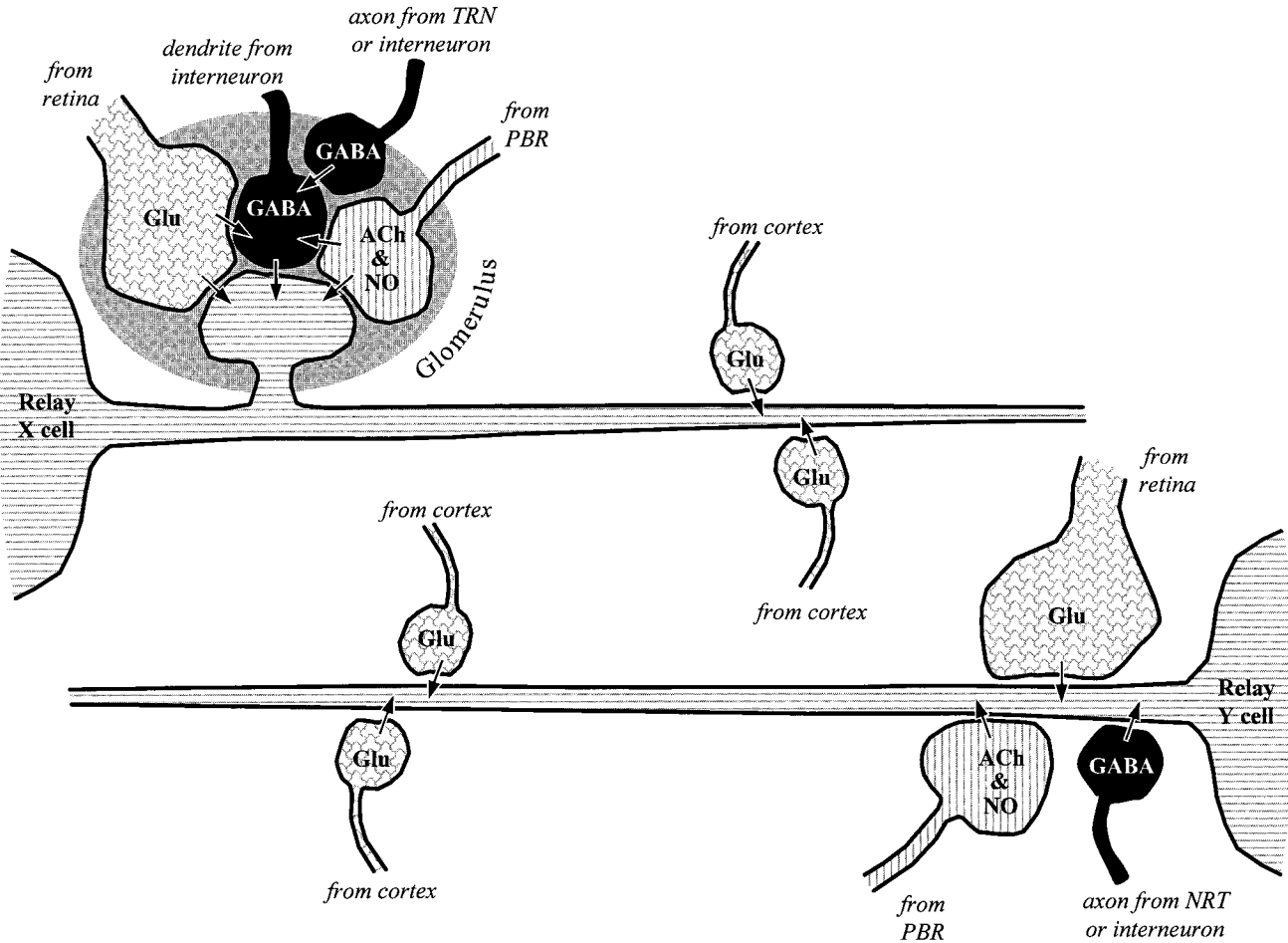


Fig. 13. Diagram showing various inputs onto dendrites of relay X and Y cells. Parabrachial terminals containing acetylcholine (ACh) and nitric oxide (NO) contact proximal dendrites in the vicinity of retinal inputs containing glutamate (Glu). This is the retinal recipient zone. These are found both within glomeruli, presumably reflecting the relay X cell pattern, and outside of glomeruli, presumably reflect-

ing the relay Y cell pattern. In glomeruli, parabrachial terminals can contact both GABAergic F2 terminals from dendrites of interneurons and the relay cell dendrite, whereas outside of glomeruli they contact only dendrites. Cortical terminals containing glutamate contact both cells only on distal dendrites in the cortical recipient zone.

methodology, such as orthograde transport to label corticogeniculate terminals and immunocytochemistry to label parabrachial terminals, different populations became evident. Raczkowski and Fitzpatrick (1989) have already shown that terminals labeled for ChAT in the lateral geniculate nucleus of the cat are on average larger than unlabeled RSD terminals, and our data confirm this finding. In addition, as Figure 12 illustrates, parabrachial terminals are larger than corticogeniculate terminals. Corticogeniculate terminals appear to be a fairly homogeneous group of smaller terminals with archetypal RSD morphology. Parabrachial terminals have a more widespread size distribution, some being sufficiently small to be considered RSD terminals, others being so large that they must be considered RLD terminals.

This means that an RSD terminal seen in unstained material cannot be unequivocally identified as a corticogeniculate terminal. The larger terminals of this type, the RLD terminals, are too large to be cortical and can thus be reasonably confidently identified as of brainstem origin, although other possible candidates cannot be completely ruled out. Although it appears that the vast majority of

brainstem terminals in the lateral geniculate nucleus of the cat contain ACh and NO and derive from the parabrachial region (present study; de Lima and Singer, 1987b; Steriade et al., 1988; Raczkowski and Fitzpatrick, 1989; Bickford et al., 1993), other types are also present in small numbers. One of these brainstem inputs derives from the pretectum, but this is GABAergic and would not be mistaken for RSD or RLD terminals (Cucchiari et al., 1991a, 1993; Wahle et al., 1994). However, other brainstem inputs include serotonergic inputs from the dorsal raphe nucleus, noradrenergic inputs from cells in the parabrachial region (these intermingle with the cells containing ACh and NO), and histaminergic inputs from the tuberomammillary nucleus of the hypothalamus (de Lima and Singer, 1987a; Uhrlich et al., 1993). It is not yet known how many terminals from these inputs exist or the extent to which these terminals have morphological characteristics that would be subsumed in the RSD plus RLD category. However, terminals of the serotonergic input have been defined, and they have morphology similar to that of RSD terminals (de Lima and Singer, 1987a). We thus have insufficient data to identify

the origins of terminals in the RSD plus RLD category unless special staining protocols are used, such as immunocytochemistry or axonal transport of labels.

Terminal location. An even more dramatic difference than that in size between corticogeniculate and parabrachial terminals is their targeted region of dendritic arbors on relay cells. Figure 13 schematically illustrates this difference. When enough of the postsynaptic dendrite could be visualized, we found that parabrachial terminals contacted the same dendritic region as retinogeniculate (RLP) terminals; this we refer to as the retinal recipient zone. Corticogeniculate terminals, in contrast, contact dendritic segments devoid of retinogeniculate terminals; this is the cortical recipient zone. Our data also suggest that any RSD terminal found in a glomerulus is a parabrachial terminal. This is because we found many such terminals in glomeruli stained for ACh and/or BNOS, but not a single one of our sample of 437 terminals labeled from visual cortex was found in a glomerulus. However, Vidnyanszky and Hamori (1994) recently reported on the distribution of corticogeniculate terminals after labeling them from cortex in a manner similar to that used in the present study. These authors report finding that these terminals "were usually extraglomerular," but that "a smaller number" were found at the periphery of glomeruli. Because the authors do not provide numbers, it is hard to determine how discrepant their observations are from ours. In any case, we cannot explain this discrepancy, but it seems safe to conclude that, if corticogeniculate terminals ever enter glomeruli, they do so exceedingly rarely.

Because previous evidence indicates that glomeruli are associated most often with relay X cells and that relay Y cells have very few glomeruli (Wilson et al., 1984; Hamos et al., 1987), these two cell types are shown in Figure 13. The implication is that the parabrachial terminals found within glomeruli represent the typical pattern for X cells, whereas the parabrachial terminals found outside glomeruli represent the typical pattern for Y cells.

We thus conclude that the segregation of dendritic arbors of geniculate cells into retinal recipient and cortical recipient zones is even more complete, with virtually no overlap, than was previously appreciated. For instance, Wilson et al. (1984) noted that RSD terminals dominated peripheral dendritic regions and that RLP (retinal) terminals were found only proximally, but considerable overlap was seen in intermediate dendritic regions that received inputs from both RSD and RLP terminals. At the time, virtually all RSD terminals were thought to be of cortical origin, so the segregation of retinal recipient and cortical recipient zones was thought to be incomplete. We can now reinterpret those data: The RSD terminals found mixed with RLP terminals in intermediate dendritic regions were probably parabrachial terminals. Furthermore, the segregation of corticogeniculate and parabrachial inputs onto the dendritic arbors of geniculate neurons is remarkably complete.

ACKNOWLEDGMENTS

We thank Olga Levin and Guadalupe Garcia for their expert technical assistance. This research was supported by USPHS grant EY03038; A.E. was supported by USPHS Postdoctoral Fellowship EY06473.

LITERATURE CITED

- Bickford, M.E., A.E. Günlük, W. Guido, and S.M. Sherman (1993) Evidence that cholinergic axons from the parabrachial region of the brainstem are the exclusive source of nitric oxide in the lateral geniculate nucleus of the cat. *J. Comp. Neurol.* 334:410–430.
- Bickford, M.E., A.E. Günlük, S.C. Van Horn, and S.M. Sherman (1994) GABAergic projection from the basal forebrain to the visual sector of the thalamic reticular nucleus in the cat. *J. Comp. Neurol.* 348:481–510.
- Burke, W., and A.M. Cole (1978) Extraretinal influence on the lateral geniculate nucleus. *Rev. Physiol. Biochem. Pharmacol.* 80:105–166.
- Cucchiari, J.B., D.J. Uhlrich, and S.M. Sherman (1988) Parabrachial innervation of the cat's dorsal lateral geniculate nucleus: An electron microscopic study using the tracer *Phaseolus vulgaris* leucoagglutinin (PHA-L). *J. Neurosci.* 8:4576–4588.
- Cucchiari, J.B., M.E. Bickford, and S.M. Sherman (1991a) A GABAergic projection from the pretectum to the dorsal lateral geniculate nucleus in the cat. *Neuroscience* 41:213–226.
- Cucchiari, J.B., D.J. Uhlrich, and S.M. Sherman (1991b) Electron-microscopic analysis of synaptic input from the perigeniculate nucleus to the A-laminae of the lateral geniculate nucleus in cats. *J. Comp. Neurol.* 310:316–336.
- Cucchiari, J.B., D.J. Uhlrich, and S.M. Sherman (1993) Ultrastructure of synapses from the pretectum in the A-laminae of the cat's lateral geniculate nucleus. *J. Comp. Neurol.* 334:618–630.
- Cudeiro, J., K.L. Grieve, C. Rivadulla, R. Rodriguez, S. Martinez-Conde, and C. Acuña (1994a) The role of nitric oxide in the transformation of visual information within the dorsal lateral geniculate nucleus of the cat. *Neuropharmacology* 33:1413–1418.
- Cudeiro, J., C. Rivadulla, R. Rodriguez, S. Martinez-Conde, C. Acuña, and J.M. Alonso (1994b) Modulatory influence of putative inhibitors of nitric oxide synthesis on visual processing in the cat lateral geniculate nucleus. *J. Neurophysiol.* 71:146–149.
- Cudeiro, J., C. Rivadulla, R. Rodriguez, S. Martinez-Conde, L. Martinez, K.L. Grieve, and C. Acuña (1996) Further observations on the role of nitric oxide in the feline lateral geniculate nucleus. *Eur. J. Neurosci.* 8:144–152.
- de Lima, A.D., and W. Singer (1987a) The serotonergic fibers in the dorsal lateral geniculate nucleus of the cat: Distribution and synaptic connections demonstrated with immunocytochemistry. *J. Comp. Neurol.* 258:339–351.
- de Lima, A.D., and W. Singer (1987b) The brainstem projection to the lateral geniculate nucleus in the cat: Identification of cholinergic and monoaminergic elements. *J. Comp. Neurol.* 259:92–121.
- de Lima, A.D., V.M. Montero, and W. Singer (1985) The cholinergic innervation of the visual thalamus: An EM immunocytochemical study. *Exp. Brain Res.* 59:206–212.
- Dinerman, J.L., T.M. Dawson, M.J. Schell, A. Snowman, and S.H. Snyder (1994) Endothelial nitric oxide synthase localized to hippocampal pyramidal cells: Implications for synaptic plasticity. *Proc. Natl. Acad. Sci. USA* 91:4214–4218.
- Fitzpatrick, D., I.T. Diamond, and D. Raczkowski (1989) Cholinergic and monoaminergic innervation of the cat's thalamus: Comparison of the lateral geniculate nucleus with other principal sensory nuclei. *J. Comp. Neurol.* 288:647–675.
- Gilbert, C.D., and J.P. Kelly (1975) The projections of cells in different layers of the cat's visual cortex. *J. Physiol. (London)* 163:81–106.
- Guillery, R.W. (1969a) A quantitative study of synaptic interconnections in the dorsal lateral geniculate nucleus of the cat. *Z. Zellforsch.* 96:39–48.
- Guillery, R.W. (1969b) The organization of synaptic interconnections in the laminae of the dorsal lateral geniculate nucleus of the cat. *Z. Zellforsch.* 96:1–38.
- Guillery, R.W. (1971) Patterns of synaptic interconnections in the dorsal lateral geniculate nucleus of cat and monkey: A brief review. *Vis. Res. Suppl.* 3:211–227.
- Hamos, J.E., S.C. Van Horn, D. Raczkowski, D.J. Uhlrich, and S.M. Sherman (1985) Synaptic connectivity of a local circuit neurone in lateral geniculate nucleus of the cat. *Nature* 317:618–621.
- Hamos, J.E., S.C. Van Horn, D. Raczkowski, and S.M. Sherman (1987) Synaptic circuits involving an individual retinogeniculate axon in the cat. *J. Comp. Neurol.* 259:165–192.
- Hartveit, E., and P. Heggelund (1995) Brainstem modulation of signal transmission through the cat dorsal lateral geniculate nucleus. *Exp. Brain Res.* 103:372–384.

- Ide, L.S. (1982) The fine structure of the perigeniculate nucleus in the cat. *J. Comp. Neurol.* 210:317-334.
- Jahnsen, H., and R. Llinás (1984a) Ionic basis for the electroresponsiveness and oscillatory properties of guinea-pig thalamic neurones in vitro. *J. Physiol. (London)* 349:227-247.
- Jahnsen, H., and R. Llinás (1984b) Electrophysiological properties of guinea-pig thalamic neurones: an in vitro study. *J. Physiol. (London)* 349:205-226.
- Jones, E.G., and T.P. Powell (1969a) Electron microscopy of synaptic glomeruli in the thalamic relay nuclei of the cat. *Proc. R. Soc. London [Biol.]* 172:153-171.
- Jones, E.G., and T.P.S. Powell (1969b) An electron microscopic study of the mode of termination of cortico-thalamic fibres within the sensory relay nuclei of the thalamus. *Proc. R. Soc. London [Biol.]* 172:173-185.
- Lu, S.-M., W. Guido, and S.M. Sherman (1993) The brainstem parabrachial region controls mode of response to visual stimulation of neurons in the cat's lateral geniculate nucleus. *Vis. Neurosci.* 10:631-642.
- Madison, D.V. (1993) Pass the nitric oxide [review]. *Proc. Natl. Acad. Sci. USA* 90:4329-4331.
- Mathes, C., and S.H. Thompson (1996) The nitric oxide/cGMP pathway complex couples muscarinic receptors to the activation of Ca^{2+} influx. *J. Neurosci.* 16:1702-1709.
- McCormick, D.A. (1992) Cellular mechanisms underlying cholinergic and noradrenergic modulation of neuronal firing mode in the cat and guinea pig dorsal lateral geniculate nucleus. *J. Neurosci.* 12:278-289.
- Montero, V.M. (1989) Ultrastructural identification of synaptic terminals from cortical axons and from collateral axons of geniculo-cortical relay cells in the perigeniculate nucleus of the cat. *Exp. Brain Res.* 75:65-72.
- Montero, V.M. (1994) Quantitative immunogold evidence for enrichment of glutamate but not aspartate in synaptic terminals of retino-geniculate, geniculo-cortical, and cortico-geniculate axons in the cat. *Vis. Neurosci.* 11:675-681.
- Pape, H.-C., and R. Mager (1992) Nitric oxide controls oscillatory activity in thalamocortical neurons. *Neuron* 9:441-448.
- Phend, K.D., R.J. Weinberg, and A. Rustioni (1992) Techniques to optimize post-embedding single and double staining for amino acid neurotransmitters. *J. Histochem. Cytochem.* 40:1011-1020.
- Raczkowski, D., and D. Fitzpatrick (1989) Organization of cholinergic synapses in the cat's dorsal lateral geniculate and perigeniculate nuclei. *J. Comp. Neurol.* 288:676-690.
- Rapisardi, S.C., and T.P. Miles (1984) Synaptology of retinal terminals in the dorsal lateral geniculate nucleus of the cat. *J. Comp. Neurol.* 223:515-534.
- Sanderson, K.J. (1971) The projection of the visual field to the lateral geniculate and medial interlaminar nuclei in the cat. *J. Comp. Neurol.* 143:101-118.
- Schuman, E.M., and D.V. Madison (1994) Nitric oxide and synaptic function. *Annu. Rev. Neurosci.* 17:153-183.
- Sherman, S.M. (1993) Dynamic gating of retinal transmission to the visual cortex by the lateral geniculate nucleus. In D. Minciacchi, M. Molinari, G. Macchi, and E.G. Jones (eds): *Thalamic Networks for Relay and Modulation*. Oxford: Pergamon Press, pp. 61-79.
- Sherman, S.M., and C. Koch (1986) The control of retinogeniculate transmission in the mammalian lateral geniculate nucleus. *Exp. Brain Res.* 63:1-20.
- Sherman, S.M., and C. Koch (1990) Thalamus. In G.M. Shepherd (ed): *The Synaptic Organization of the Brain*, 3rd Ed. New York: Oxford University Press, pp. 246-278.
- Singer, W. (1977) Control of thalamic transmission by corticofugal and ascending reticular pathways in the visual system. *Physiol. Rev.* 57:386-420.
- Steriade, M., D. Paré, A. Parent, and Y. Smith (1988) Projections of cholinergic and non-cholinergic neurons of the brainstem core to relay and associational thalamic nuclei in the cat and macaque monkey. *Neuroscience* 25:47-67.
- Szentágothai, J., J. Hátori, and T. Tömböl (1966) Degeneration and electron microscope analysis of the synaptic glomeruli in the lateral geniculate body. *Exp. Brain Res.* 2:283-301.
- Tusa, R.J., L.A. Palmer, and A.C. Rosenquist (1978) The retinotopic organization of area 17 (striate cortex) in the cat. *J. Comp. Neurol.* 177:213-236.
- Tusa, R.J., A.C. Rosenquist, and L.A. Palmer (1979) Retinotopic organization of areas 18 and 19 in the cat. *J. Comp. Neurol.* 185:657-678.
- Uhlrich, D.J., K.A. Manning, and T.P. Pienkowski (1993) The histaminergic innervation of the lateral geniculate complex in the cat. *Vis. Neurosci.* 10:225-235.
- Uhlrich, D.J., N. Tamamaki, P.C. Murphy, and S.M. Sherman (1995) Effects of brainstem parabrachial activation on receptive field properties of cells in the cat's lateral geniculate nucleus. *J. Neurophysiol.* 73:2428-2447.
- Van Horn, S.C., J.E. Hamos, and S.M. Sherman (1986) Ultrastructure of the intrageniculate axon collateral of a projection neuron in the cat. *Soc. Neurosci. Abstr.* 12:1037.
- Vidnyanszky, Z., and J. Hátori (1994) Quantitative electron microscopic analysis of synaptic input from cortical areas 17 and 18 to the dorsal lateral geniculate nucleus in cats. *J. Comp. Neurol.* 349:259-268.
- Wahle, P., V. Stuphorn, M. Schmidt, and K.-P. Hoffmann (1994) LGN-projecting neurons of the cat's pretectum express glutamic acid decarboxylase mRNA. *Eur. J. Neurosci.* 6:454-460.
- Wang, S.Z., S.Z. Zhu, and E.E. el-Fakahany (1994) Efficient coupling of m5 muscarinic acetylcholine receptors to activation of nitric oxide synthase. *J. Pharmacol. Exp. Ther.* 268:552-557.
- Weber, A.J., R.E. Kalil, and M. Behan (1989) Synaptic connections between corticogeniculate axons and interneurons in the dorsal lateral geniculate nucleus of the cat. *J. Comp. Neurol.* 289:156-164.
- Wilson, J.R., M.J. Friedlander, and S.M. Sherman (1984) Fine structural morphology of identified X- and Y-cells in the cat's lateral geniculate nucleus. *Proc. R. Soc. London [Biol.]* 221:411-436.